Indian J.Sci.Res.3 (1): 148-172, 2014 ISSN : 0976-2876 (Print)
ISSN : 2250-0138 (Online)

THERMODYNAMIC ASSESSMENT OF A HYBRID SOFC/GT CYCLE CONSIDERING OXY-ANODE COMBUSTION CO_2 CAPTURE TECHNOLOGY

GH. ARAB [a], H. GHADAMIAN [b 1], M. KHALAJI ASSADI [a], R. ROSHANDEL [c] AND H. FARZANEH [a]

[a] Department of Energy Engineering, College of Energy and Environment, Tehran Science and Research Branch, Islamic Azad University, Tehran, Iran.
[b] Department of Energy, Materials and Energy Research Center (MERC), Tehran, Iran.
[c] Department of Energy Engineering, Sharif University of Technology, Azadi ave., Tehran, Iran.

ABSTRACT

Integrating new power generation technologies with environmental considerations lead improving performance and developing high efficient systems that is contributed to minimizing emissions. To achieve this goal, in this research, an energy & exergy analysis is introduced as a preliminary step for a hybrid SOFC/GT base power plant with CO_2 capture and waste heat recovery system. The proposed combined cycle includes an internal reforming tubular SOFC fed with methane, likewise a CO_2 capture system based on oxy-anode combustion and HRSG is added to provide saturated steam. For the mentioned subsidiaries, considering total site efficiency improvement enables application capacity of a green attractive low CO_2 emission plant, if it pays enough in attention about a bit miss in efficiency, regarding CO_2 capture. With the application of open source code software based on a steady state process, a zero dimensional model is developed and the thermodynamic properties of the most significant streams of the plant are also proposed. To achieve this goal, the energy & exergy streams' specifications are performed for all involved components. Additionally, the highest proportion of irreversibility is identified and prioritized. Meanwhile the designated model is validated with the similar conditions reported in the literature. For bench marking purposes, a complementary parametric study is also performed to show the effects of important variations & values on system operation characteristics. The final results identify for CO_2 capture purpose, the loss opportunity for 516.84 MWh per year electricity productions against with 5342.20 tCO_2 gain annually. The result of quantitative analysis also explains specific CO_2 production in this cycle is 310.98 g kWh^{-1} that shows considerable gains compare with other references. Final conclusions demonstrate that the proposed systems have enough capability to be applied within industries instead of conventional low efficiency and highly pollutant systems currently marked at the market.

Keywords: CO_2 capture; Energy efficiency; Exergy analysis; Parametric study.

According to the latest statistics provided by the IEA, global electricity production in 2010 was 21431 TWh in which the main part of this electricity is provided and prioritized by coal and gas fueled power plants (IEA, 2013). The last but not the least of the consequences for applying these technologies related to power generation is environmental pollution aspects.

SOFCs are currently being demonstrated in sizes from 1 kW up to 250 kW plants, with plans to reach the multi-MW range. SOFCs utilize a non-porous metal oxide (usually Yttria-stabilized zirconia, Y_2O_3-stabilized ZrO_2) electrolyte material. SOFCs operate between 650 and 1000°C, where ionic conduction is accomplished by oxygen ions ($O^{=}$) (NFCRC, 2013). Typically the anode of an SOFC is cobalt or nickel zirconia (Co-ZrO_2 or Ni-

[1] Corresponding author: h.ghadamian@merc.ac.ir

ZrO_2) and the cathode is strontium-doped lanthanum manganite (Sr-doped $LaMnO_3$) (Singhal, 2000). SOFC is capable of using gaseous fuels like natural gas or liquefied ethanol and solid coal depending on availabilities. It can also provide any power production contributed to power plants, transportation and residential applications. Generally, efficiencies of fuel cells are considerable high, when it compares with heat engines. Meanwhile, recent efforts to achieve a clean technology with high efficiency of power generation have provided a path for development of technologies such as hybrid SOFC/GT. This hybrid power plant cycle using SOFC has several advantages such as high electrical efficiency, high power density, low emissions, low noise and the ability to synchronize with alternative fuels (Singhal, 2000). Moreover, the mature and commercial gas turbine technology has led to the development of high electrical efficiency that has economical merits. As an advice, it is important to mention that using CHP technology in downstream cycles can prepare more efficient use of energy in relation with whole overview of the site. Achieving the total efficiency of 86 %, reported already, has been related to the aforementioned advice (Palsson et al., 2000).

Countries around the world are developing interests in the high-efficiency hybrid cycles (Fuel cell handbook, 2004). The Siemens Power Corporation hybrid tubular SOFC /micro turbine generator was built and tested at the National Fuel Cell Research Center (NFCRC), in Irvine, California. In this test the hybrid direct gas turbine fuel cell topping cycle configuration was demonstrated. This test includes pressurization of the fuel cell to provide a total of 220 kW of power regarding with the hybrid system. Test results proved that high efficiency and ultra-low emissions was achievable with these types of hybrid cycles, but integration of process & proper operation are considerably in troubles, with such kind of hybrid systems. The system operated for over 2900 hours and produced up to 220 KW at fuel-to-electricity conversion efficiencies of up to 53% (Dennis, 2007).

Developers are targeting both the low and high power ranges. G.j. Williams *et al.*, studied the description of the different hybrid configurations and their contributed results explained the potential electrical efficiencies approaching 70% in combination SOFC with gas turbines (Williams et al. 2001). S.H. Chan *et al.*, are examined the energy and exergy analysis of a simple SOFC power system (Chan et al., 2002). F. Calise *et al.*, are discussed the simulation and exergy analysis of a hybrid SOFC/GT power system and the results provided that, for a 1.5 MW system, an electrical efficiency close to 60% and when heat loss recovery is also taken into account, a global efficiency of about 70% is achieved (Calise et al., 2006). A.V. Akkaya *et al.*, are discussed the exergetic performance coefficient analysis of a simple fuel cell system (Akkaya et al., 2007). Y. Haseli *et al.*, are examined the thermodynamic modelling of a GT/SOFC and their final conclusions, estimate that equal to 60% of the irreversibility takes place in the combustor and SOFC (Haseli et al., 2008). M. Gandiglio *et al.*, are discussed the thermo economic analysis of large atmospheric and pressurized SOFC plants and both exergetic and economic advantages result from the adoption of a pressurized SOFC/GT cycle in the framework of future advance power plants based on high temperature fuel cells (Gandiglio et al., 2013). D. Saebea *et al.*, are examined the analysis of a pressurized SOFC/GT hybrid power system with cathode gas recirculation (Saebea et al., 2013).

As well, D.M. Murphy *et al.*, explored strategies for biogas reforming and the results indicated that SOFC electrochemical performance under biogas reformate varies substantially with reforming approach (Murphy et al., 2012). H.A. Ozgoli *et al.*, studied the alternative fuels in a

hybrid gasification SOFC/GT cycle and the results indicated that the bagasse and wood chips had the total exergy efficiency of 54.5%, 57.1% in trade-off point respectively (Ozgoli et al., 2012).

R.S. Kempegowda *et al.*, presented a cost modeling approach and the economic feasibility for SOFC/GT plant configurations operating under three scenarios, their results indicated that the cost of the steam gasification system is the highest compared with other similar systems due to the hydrogen production (Kempegowda et al., 2012). H. Ghadamian *et al.*, also investigated thermo-economic analysis of absorption air cooling system for pressurized SOFC/GT cycle, the assessment indicated that appending an absorption, inlet air cooling system will result in maximization combined cycle efficiency and outlet power and the payback period was to equal 8.1 year, that seems suitable in the power cycles point of view (Ghadamian et al., 2012).

Whenever natural gas is used as a feed, carbon removal technology is a common word due to the SOFC nature that produces CO_2. Different CO_2 capture technologies can be proposed and one of this categorization has been presented by J.W. dijkstra & D. Jansen which is based on the SOFC technologies (dijkstra et al., 2002). Bredesen *et al.*, has proposed another categorization that focuses on ITM which works at high temperatures (800-900^{o}C) (Bredesen *et al.*, 2004). H.M. Hanne *et al.,* are discussed different CO_2 capture cycles for GT systems have been compared and then concluded that the GT/SOFC system has the highest total efficiency (67.3%) (Hanne et al., 2007). Franzoni et al., performed a thermodynamic analysis based on three comparing cycles including the basic cycle, cycles with CO_2 capture system using pre-combustion, and oxy-fuel combustion system. Their results consider increase in the total investment cost for the amine separation plant is accompanied by a significant net efficiency decrease, causing a high cost of emissions. Apart from that, they concluded the implementation of the carbon dioxide separation by condensation of the exhaust streams appears to be really attractive in terms of efficiency and costs (Franzoni et al., 2008). T. Kuramochi *et al.*, showed that the use of SOFC in the CO_2 market is an attractive option from the economic point of view (Kuramochi et al., 2009). S.K. Park *et al.*, has also confirmed that CO_2 absorption system adds up with hybrid SOFC/GT relate to high efficiency and low emissions is achievable as a fact (Park et al., 2011). Proper classification of the different cycle structures in CO_2 capture systems is presented with the focus on three different technological configurations (Pre-combustion, Post combustion and Oxy-combustion) and their results demonstrate suitable applications (Hill, 2003). J. Meyer *et al.*, in order to develop clean power generation technologies, by using sorption-enhanced steam methane reforming process (SE-SMR) and Zero Emission Gas power concept (ZEG), efficiency of 77% as well as complete CO_2 capture have been achieved (Meyer et al., 2011). T.A. Adams *et al.*, are presented a review of energy conversion systems which engaged with SOFCs as their primary electricity generation component. The systems reviewed are largely geared for development and use in the short and long-term future. These include systems for bulk power generation, distributed power generation, and systems integrated with other forms of energy conversion such as fuel production. The potential incorporation of CO_2 capture and sequestration technologies and the influences of potential government policies are also discussed (Adams et al., 2013). Global research about CO_2 capture technologies are moving toward oxy-anode combustion and much research are in progress to develop economic and efficient methods of oxygen production. Furthermore oxy-anode combustion, as an efficient method to fully CO_2 capture with high efficiency, is the best method for these hybrid cycles, at present time (Arab et al., 2013).

There can be many different cycle configurations for the hybrid fuel cell/turbine plant (Fuel cell handbook, 2004). Hybrid system modeling, as an active field of research is conducted with different objectives such as configuration analysis, simulation, optimization, and parametric analysis and there are not a few research that are being performed for modeling regarding CO_2 capture integrated to SOFC/GT cycle. Surveys and studies in this field have been performed mostly in relation with the cycle energy balance and conservation point of view and less attention is being paid to exergy analysis which can get useful comparative results. Therefore, in this study, a basic cycle SOFC/GT (layout 1) is modeled and examined first. After validating the model, the layout 2 is introduced that includes CO_2 capture system using oxy anode combustion technology based on previous findings (Kutas, 1995). The added impact of the technology on cycle is studied afterwards. The system is modeled using EES open source code software regarding mass, energy, exergy and electrochemical equations. The model is solved simultaneously. In the next step, a parametric analysis is performed to determine most influential parameters. Design insights of fuel cell systems can be considerably improved when conventional energetic analyses are supplemented with exergetic analyses and as a positive point of view, by introducing the Exergetic Performance Coefficient (EPC), the exergetic analysis is carried out for the cycles in this paper.

CYCLES DESCRIPTION

In SOFC module, fuels' chemical energy directly converts into electrical energy through electrochemical reactions. GT modules also provide the required air pressure and temperature that enters SOFC module, causing the turbine to generate additional power and finally regarding HRSG modules using waste heat from the turbine. The layout 1 of the SOFC/GT cycle is presented in figure 1. This cycle includes an SOFC stack with internal reformer, gas turbine with recuperator and a HRSG to produce steam. Fuel enters the fuel compressor and then with the anode recirculation fuel enters the pre-reformer and finally to the fuel cells' anode. On the other side, air enters the cycles and after being compressed in a compressor, with two stages of preheating, enters the fuel cells' cathode. Part of the anode's off-gas is burned with the air from cathode outlet just as after-burner and flue gases pass through the recuperator that enters the gas turbine to produce power. After preheating the input air in recuperator, flue gases pass through the HRSG (stream No. 16). It has sufficient temperature to produce valuable steam that would be used for various applications such as process heating.

Nomenclature

E_{act}	Activation energy (kJ mol^{-1})	*Subscripts and Superscripts*	
A_{act}	Cell active area (m^2)	act	Activation
i	Cell current density (A m^{-2})	an	Anode
w	Cell width	ca	Cathode, Air Compressor
P_{SOFC}	DC SOFC power (kW)	ch	Chemical
K_p	Equilibrium constant	conc	Concentration
$\dot{Ex}$	Exergy (kW)	inv	DC/AC inverter
F	Faraday constant (96 485 As mol^{-1})	D	Destruction
U_f	Fuel utilization factor	el	Electrolyte
G	Gibbs energy (kJ kmol^{-1})	g	Generator
$\dot{n}$	H_2 reacted moles (mol s^{-1})	in	Interconnector, Inlet

$\dot{Q}$	Heat transfer rate (kW)	is	Isentropic
i_L	Limited current density (A m^{-2})	m	Mechanical
LHV	Lower heating value (kJ mol^{-1})	Ohm	Ohmic
$\dot{m}$	Mass flow rate (g s^{-1})	Out	Outlet
$\dot{n}_i$	Molar flow rate (mol s^{-1})	ph	Physical
M	Molecular weight (kg $kmol^{-1}$)	rec	Recuperator
E_{re}	Nernst voltage (V)	0	Reference condition
N_{cell}	Number of cells	t	Ton, Turbine, Total
n_e	Number of electrons	*Abbreviation*	
V	Overvoltage (V)	A.B	After Burner
DT_p	Pinch point temperature difference (K)	ASU	Air Separation Unit
$\dot{W}$	Power (kW)	CHP	Combined Heat and Power
P	Pressure (bar)	Eco	Economizer
RP	Pressure ratio	EES	Engineering Equation Solver
d	SOFC diameter (cm)	EPC	Exergetic Performance Coefficient
ex	Specific exergy	Eva	Evaporator
h	Specific molar enthalpy (kJ $kmol^{-1}$)	GT	Gas Turbine
s	Specific molar entropy (kJ (kmol.K) $^{-1}$)	HPR	Heat to Power Ratio
SCR	Steam to carbon ratio	HRSG	Heat Recovery Steam Generator
T	Temperature (K)	IEA	International Energy Agency
R_u	Universal gas constant (kJ (kmol.K) $^{-1}$)	SOFC	Solid Oxide Fuel Cell
Greek symbols			
α	Charge transfer coefficient		
ε	Effectiveness		
η	Efficiency		
y_i	Mole fraction		
δ	Thickness		

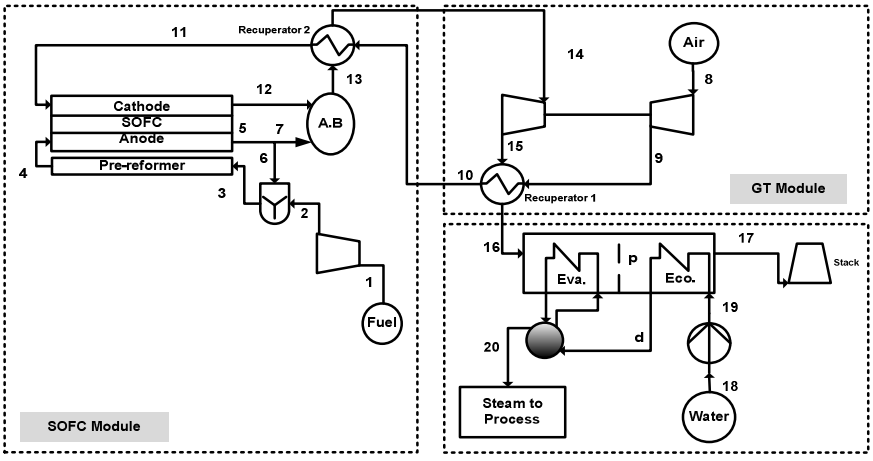

Figure 1- *A schematic view of a methane-fuelled SOFC/GT cycle with internal reformer and anode off-gas recirculation (layout 1)*

CO_2 capture module has been performed by oxy anode combustion method with regards to layout 2. Figure 2 shows a schematic of this module that includes the layout 1 within the CO_2 capture module. To provide maximum recovered heat, re-arrangement of recuperators is performed. In proposed cycle, a part of the anode's off-gas is recycled to complete the process of reforming in pre-reformer and the remaining part is burned directly with pure oxygen instead of air at after burner. The stream line No. 22 includes CO_2, water content and bit oxygen. Water will be separated with cooling & condensing afterwards. The CO_2 and oxygen mixture will enters a section named inter-cooling compression up to 90 bar pressure, for separation purpose (Kuramochi et al., 2009). Depleted air from cathode outlet after crossing through the recuperator enters the turbine and eventually is discharged to the atmosphere.

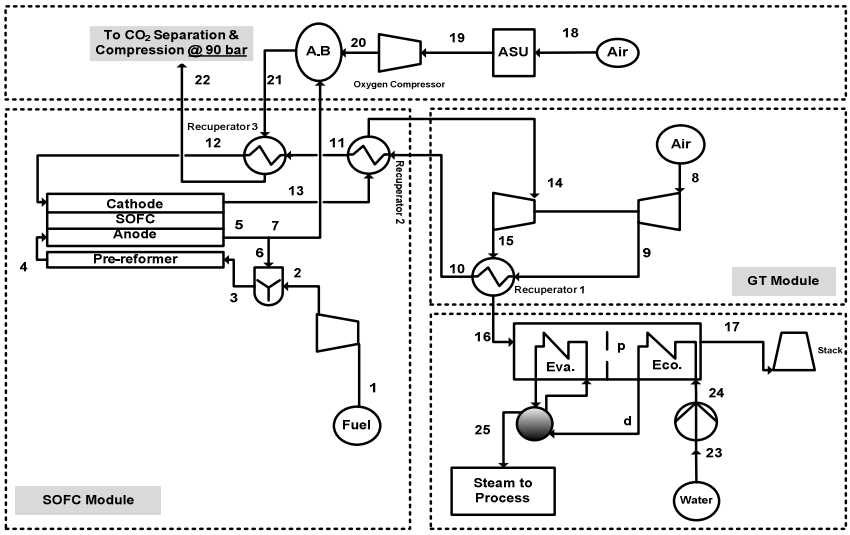

Figure 2- *Designed cycle within CO_2 capture module (layout 2)*

MODELING METHODOLOGY

A complex form of solving model equations including electrochemical reactions, mass, energy and exergy equations balances for the convergence of model results was developed. Computational models give us molar flow values ($\dot{n}_i$) and mole fraction (y_i) along with all the physical properties such as enthalpy, entropy, pressure and temperature of the streams. The assumptions are as follows:

1- System components are taken as a lumped control volume,

2 - Equipment work in steady state conditions,

3 - Chemical reactions proceed to equilibrium states,

4 - All gases are assumed to be ideal state.

EXERGY MODELING

Considering a specified energy system in term of exergy analysis depends on the location and the amounts of exergy losses. The goal of this analysis is to identify the location, type and the amount of entropy production during various thermodynamic processes and to understand the contributing factors affecting the system during production of these irreversibilities, as the loss values contributed to entropies. In this way, in addition to evaluating the performance of various components, solutions to increase efficiencies can be identified. When the effects of fields like magnetic, electrical and surface tension are negligible, the specific exergy (ex), is obtained from equation (1-a) (Haseli et al., 2008). In the mentioned cycles, like similar studies in the literature, the potential and kinetic exergy are

[1] Corresponding author: h.ghadamian@merc.ac.ir

negligible. As a result, the physical exergy can be obtained from equation (1-b). The chemical exergy is a maximal achievable work when the system states at T_0 and P_0 until it gets to a chemical equilibrium with the environment. Therefore, to calculate the chemical exergy, not only temperature and pressure should be known, but also the chemical composition of the streams must be specified as well. Chemical exergy of an ideal gas mixture is calculated according to equation (1-c). It is known that if the ambient temperature is T_0 and y_k is mole fraction of ks' element then ex_k^{CH} is the standard molar chemical exergy for ks' element that is used for various materials (Akkaya et al., 2008).

$$ex = ex^{PH} + ex^{ke} + ex^{pe} + ex^{ch} \quad (1\text{-a})$$

$$ex^{PH} = (h - h_0) - T_0(s - s_0) \quad (1\text{-b})$$

$$ex^{ch} = \sum y_k\, ex_k^{Ch} + R_u T_0 \sum y_k \ln y_k \quad (1\text{-c})$$

$$\dot{Ex}_D = \sum_j \dot{Q}_j \left(1 - \frac{T_0}{T_j}\right) - \dot{W} + \sum_i (\dot{Ex}_i)_{in} - \sum_i (\dot{Ex}_i)_{out} \quad (1\text{-d})$$

$$\dot{Ex}_{D,Total} = \sum_i \dot{Ex}_{D,i} \quad (1\text{-e})$$

$$EPC_{cycle} = \left(1 - \frac{\dot{E}x_{D,total}}{\dot{E}x_{fuel,in}}\right).100 \quad (1\text{-f})$$

By this mean, the exergy destruction rate in each control volume is calculated based on the general equation (1-d) and the total amount of exergy destruction in cycle is calculated using equation (1-e). The EPC is a novel concept introduced in this research to accumulate all-in-one about exergetic patterns of cycle presented in equation (1-f). The EPC indicator is an explanation of exergy destruction effects in a system. In other words, this EPC shows which layout cycle is worse than the other in comparison of exergy destructions. This includes a parallel meaning with the saving in useful potential of exergy, which named heat & power. In fact, increasing in EPC will explain a suitable awareness about energy media in a system.

SOFC MODULE MODELING

This module includes the fuel compressors, mixer, pre-reformer, ejector, tubular SOFC and AC/DC inverter, in which the specifications are obtained from references (Kuramochi et al., 2009, Hill, 2003, Bavarsad, 2009). The methane is used as an inlet fuel which passes after crossing the fuel compressor. It then enters the mixer and is blended with anode's off-gas fuel. As an advantage, off-gas fuel from anode side includes steam and heat energy for the fuel reforming process. Therefore, part of it was returned by an ejector and is added to the input fuel. Amount of diluted returned fuel can be achieved from equation (2) according to the steam-carbon ratio, as a demand. In order to have a proper function for pre-reformer system, the mentioned ratio is guessed and usually rated between 2 to 3 (non-dimensional value).

$$SCR = \frac{\dot{n}_{3,H_2O}}{\dot{n}_{3,CH_4}} \quad (2)$$

Outlet fuel of the mixer enters the pre-reformer and the reforming and shifting reactions occur as mentioned in equations (3) and (4). Based on inherent behaviors related to the mentioned shift reactions, the inlet methane and carbon monoxide are partly converted to hydrogen. It should be noted that, the reaction is assumed to state at chemical equilibrium and the equilibrium temperature of the pre-reformer is considered equal to the outlet temperature (T_4).

$$CH_4 + H_2O \rightarrow CO + 3H_2 \quad (3)$$

$$CO + H_2O \rightarrow CO_2 + H_2 \quad (4)$$

The amount of the reformed methane and shifted carbon monoxide and the composition of the outlet mixture are obtained by using the equilibrium constant equations (5) and (6). The equilibrium constants and thermal functions are called Kp_r and Kp_s respectively and are obtained based on the temperature relations of the equations (7) and (8). The nominated coefficients are available, referred as (a_1, a_2 … a_{10}) based on reference (Motahar et al., 2009). It is assumed that the required heat energy of the pre-reformer is provided by SOFC fuel cell stack.

$$Kp_r = \frac{p_{H_2}^3 \cdot p_{CO}}{p_{CH_4} \cdot p_{H_2O}} \quad (5)$$

$$Kp_s = \frac{p_{H_2} \cdot p_{CO_2}}{p_{CO} \cdot p_{H_2O}} \quad (6)$$

$$\ln(Kp_r) = a_1T^4 + a_2T^3 + a_3T^2 + a_4T + a_5 \quad (7)$$

$$\ln(Kp_s) = a_6T^4 + a_7T^3 + a_8T^2 + a_9T + a_{10} \quad (8)$$

Outlet gases from pre-reformer enter the fuel cell with internal reformer and the reactions provided in the equations (3), (4) and (9) occur simultaneously. It is assumed that the whole methane entering SOFC is completely reformed and exhausted gases do not contain any methane. In this way, the amount of consumed hydrogen is obtained by equation (10). SOFC cell voltage is calculated according to equation (11) in which E_{re} is given by the Nernst equation (12). The V_{act} is obtained based on the Butler–Volmer equation using equations (13a, b, and c). Based on the thermal resistance of each connection the total ohmic polarization named V_{ohm}, related to anode (14-a), cathode (14-b), electrodes (14-c) and inter connector (14-d) is calculated using equation (14-e). It's also notified, for concentration losses called V_{conc}, the calculation is based on equation (15). The required information to calculate voltage drops are presented in table 1 (Motahar et al., 2009). With further calculations, the output DC and AC power of the SOFC could be obtained using equations (16) and (17).

$$H_2 + \frac{1}{2}O_2 \rightarrow H_2O \quad (9)$$

$$U_f = \frac{\dot{n}}{4\dot{n}_{1,CH_4}} \quad (10)$$

$$V = E_{re} - V_{act} - V_{ohm} - V_{conc} \quad (11)$$

$$E_{re} = -\frac{\Delta G^0}{n_eF} - \frac{\Delta G}{n_eF} = -\frac{\Delta G^0}{n_eF} + \frac{R_uT}{n_eF}\ln\left(\frac{p_{H_2}p_{O_2}^{1/2}}{p_{H_2O}}\right) \quad (12)$$

$$i = i_0\left\{\exp\left(\alpha\frac{n_eF}{R_uT}V_{act}\right) - \exp\left[-(1-\alpha)\frac{n_eF}{R_uT}V_{act}\right]\right\}, \alpha = 0.5 \quad (13\text{-a})$$

$$i_{0,an} = \gamma_{an}\left(\frac{p_{H2}}{p_0}\right)\left(\frac{p_{H2o}}{p_0}\right)\exp\left(-\frac{E_{act,an}}{R_uT}\right) \quad (13\text{-b})$$

$$i_{0,ca} = \gamma_{ca}\left(\frac{p_{O_2}}{p_0}\right)^{0.25}\exp\left(-\frac{E_{act,ca}}{R_uT}\right) \quad (13\text{-c})$$

$$V_{ohm,an} = \frac{i\rho_{an}(A\pi d)^2}{8\delta_{an}} \quad (14\text{-a})$$

[1] Corresponding author: h.ghadamian@merc.ac.ir

$$V_{ohm,ca} = \frac{i\rho_{ca}(\pi d)^2}{8\delta_{ca}} A[A + 2(1 - A - B)] \quad (14\text{-b})$$

$$V_{ohm,el} = i\rho_{el}\delta_{el} \quad (16\text{-c})$$

$$V_{ohm,in} = i(\pi d)\rho_{in}\frac{\delta_{in}}{w_{in}} \quad (14\text{-d})$$

$$\rho = a \,.\, \exp(\frac{b}{T}) \quad (14\text{-e})$$

$$V_{conc} = -R_u T \frac{\ln(1 - \frac{i}{i_L})}{n_e F} \quad (15)$$

$$P_{SOFC} = \frac{N_{cell} \,.\, V \,.\, i \,.\, A_{act}}{1000} \quad (16)$$

$$\dot{W}_{SOFC} = \eta_{inv} \,.\, P_{SOFC} \quad (17)$$

Table 1- *constant parameters for voltage loss*

Activation voltage			
$\gamma_{ca}(A\,m^{-2})$	1.49 e10		
$\gamma_{an}(A\,m^{-2})$	2.13 e8		
$E_{act,ca}(kJ\,mol^{-1})$	160		
$E_{act,an}(kJ\,mol^{-1})$	110		
Ohmic voltage	**a**	**b**	**γ (µm)**
Anode	2.98 e-5	-1392	100
Cathode	8.11 e-5	600	2200
Electrolyte	2.94 e-5	10350	40
Interconnector	1.256 e-5	4690	100
SOFC diameter	2.2 (cm)		
Active length	150 (cm)		
A (geometric constant)	0.13		
B (geometric constant)	0.804		

GAS TURBINE MODULE MODELING

Gas turbine module contains compressors, turbine, after burner and recuperators. The air before entering the SOFC is preheated up to fuel cells' operating temperature. Cycle compressors are modeled by using equations of state between working pressure ratio and isentropic efficiency of the compressor. Equations (18) and (19) are provided for the air compressors in layout 1 and can be applied for fuel and oxygen compressors. For the turbine, the same method is applied for the modeling. It is based on pressure ratio equations (20) and isentropic efficiency (21). Due to the mechanical coupling system performance and efficiency of the generator, the power output of the GT module is calculated by equation (22). Recuperators considerations are taking place by means of effectiveness used within equation (23) and also presented recuperator 1 at layout 1. Continually by the given value of ε_{rec}, the recuperators' cold flow outlet temperature is calculated. Based on energy balance, the hot outlet flow temperature is calculated then. This method is applied for all of the recuperators' sub-model processing.

$$P_9 = P_8 \,.\, RP_{ca} \tag{18}$$

$$\eta_{is,ca} = \frac{h_{9,is} - h_8}{h_9 - h_8} \tag{19}$$

$$P_{14} = P_{15} \,.\, RP_t \tag{20}$$

$$\eta_{is,t} = \frac{h_{14} - h_{15}}{h_{14} - h_{15,is}} \tag{21}$$

$$\dot{W}_{GT} = \dot{W}_T \,.\, \eta_m \,.\, \eta_g - \dot{W}_{ca} \tag{22}$$

$$\varepsilon_{rec1} = \frac{T_{10} - T_9}{T_{15} - T_9} \tag{23}$$

HRSG MODELING

HRSG module affects on the overall cycles profile. Recuperators' exhausted gas flow has the capability to produce steam. Referring to figure 3; HRSG includes two sub systems named economizer and evaporator. Water is pressurized as much as required to feed into HRSG system and is then heated up by the hot gases flow stream in the economizer to the saturation temperature named T_d. It then enters the evaporator and the saturated steam is produced to complete the process. It should be concerned that, DT_p is the minimum temperature difference between the hot gas temperature and pinch point temperature of water at the saturation point and is obtained using equation (24). Flow rate of steam production and the terms of the output of the HRSG are taken by energy balance equations contributed to economizer and evaporator sections. For instance, in the layout 1, flow of steam generated in the evaporator $\dot{n}_{20}$ is obtained using the energy balance equation based on (25-a). Where $h_{d,w}$ is the enthalpy of saturated liquid at the evaporator inlet. By developing the energy balance equation in the economizer section of HRSG, h_{17} and T_{17} are obtained using equation (25-b).

$$T_p = T_d + DT_p \tag{24}$$

$$\left[\sum_i \left(\dot{n}_{16,i} h_{16,i}\right) + \dot{n}_{d,w} h_{d,w}\right]_{in} - \left[\sum_i \left(\dot{n}_{p,i} h_{p,i}\right) + \dot{n}_{20} h_{20}\right]_{out} = 0 \tag{25-a}$$

$$\left[\sum_i \left(\dot{n}_{p,i} h_{p,i}\right) + \dot{n}_{19} h_{19}\right]_{in} - \left[\sum_i \left(\dot{n}_{17,i} h_{17,i}\right) + \dot{n}_{d,w} h_{d,w}\right]_{out} = 0 \tag{25-b}$$

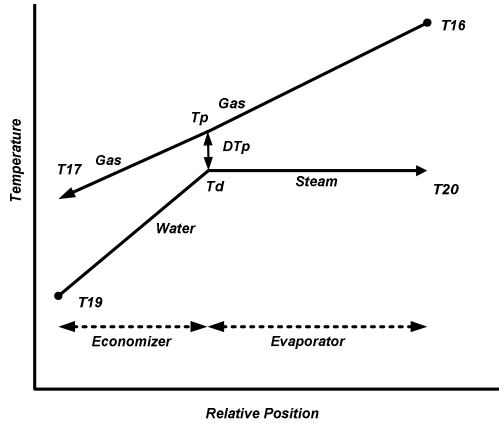

Figure 3- *HRSG flow diagram*

[1] Corresponding author: h.ghadamian@merc.ac.ir

By further calculation, the LHV basis electrical and total efficiency of the cycles could be obtained using equations (26) and (27). Also the heat to power ratio (HPR) is obtained using equation (28).

$$\eta_{ele} = \frac{\dot{W}_{net}}{\dot{n}_{CH4} . LHV} \quad (26)$$

$$\eta_{t} = \frac{\dot{W}_{net} + \dot{Q}_{HRSG}}{\dot{n}_{CH4} . LHV} \quad (27)$$

$$HPR = \frac{\dot{Q}_{HRSG}}{\dot{W}_{net}} \quad (28)$$

RESULTS AND DISCUSSION

To promote the simulation and modeling, it is necessary to define the model scope and its boundaries. In order to complete the model verifications, the input parameters and assumptions for system modeling should be define. Those are presented in table 2.

Table 2- *Models assumptions (fuel cell handbook, 2004, Haseli et al., 2008, Motahar et al., 2009)*

Parameter	Value	Parameter	Value
Reference temperature (K)	298.15	**Gas turbine module**	
Reference pressure (bar)	1.013	Air compressor isentropic efficiency (%)	78
SOFC module		Turbine isentropic efficiency (%)	82
Air utilization factor (%)	0.25	Turbine pressure ratio	2.44
Fuel utilization factor (%)	85	Air compressor pressure ratio	2.9
Steam to carbon ratio (SCR)	3	Generator .mechanical efficiency (%)	96
Average current density (A m^{-2})	3200	Recuperator pressure loss (%)	2
SOFC pressure loss (%)	2	**HRSG**	
Number of cells	9456	Minimum temperature difference (K)	20
Cell active area (m^2)	0.0834	HRSG pressure loss (%)	5
AC/DC inverter efficiency (%)	94	Steam pressure (bar)	8
Fuel compressor isentropic efficiency (%)	85	**SOFC/GT /CO_2 capture cycle**	
Fuel compressor pressure ratio	2.9	Oxygen compressor pressure ratio	2.7
Limited current (A m^{-2})	7500	CO_2 compression pressure (bar)	90

MODELING PROCESS AND RESULTS

The results of the simulation at different points of cycles are presented in the table 3 and table 4. In these tables, physical properties such as temperature, pressure, mass flow rate, exergy and the percentage of molar coefficients for all flows are presented. The results show that in design conditions of the layout 1, the cycle's electrical and total efficiencies conducted at 63.47 % and 77.67 %, respectively.

[1] Corresponding author: h.ghadamian@merc.ac.ir

Table 3- *Results for layout 1*

Stream	T (k)	P (bar)	ṁ (gs^{-1})	Ėx (kW)	Molar fraction (%)						
					CH_4	CO	CO_2	H_2	H_2O	N_2	O_2
1	298.2	1.01	61.6	3221.00	100	0	0	0	0	0	0
2	390.7	2.94	61.6	3232.00	100	0	0	0	0	0	0
3	988.8	2.88	568.4	4891.32	15.13	5.78	22.51	11.2	45.38	0	0
4	850.0	2.88	568.4	4994.60	8.2	9.85	20.75	26.6	34.6	0	0
5	1128.2	2.76	777.9	2616.23	0	6.81	26.52	13.19	53.48	0	0
6	1128.2	2.76	506.8	1704.65	0	6.81	26.52	13.19	53.48	0	0
7	1128.2	2.76	271.0	911.58	0	6.81	26.52	13.19	53.48	0	0
8	298.2	1.01	3595.4	16.02	0	0	0	0	0	79	21
9	432.9	2.94	3595.4	431.31	0	0	0	0	0	79	21
10	789.4	2.88	3595.4	1106.40	0	0	0	0	0	79	21
11	1023.0	2.82	3595.4	1736.52	0	0	0	0	0	79	21
12	1128.2	2.76	3385.9	1938.19	0	0	0	0	0	83.38	16.62
13	1258.0	2.71	3657.0	2648.97	0	0	3	0	5.99	76.63	14.38
14	1046.7	2.66	3657.0	1938.50	0	0	3	0	5.99	76.63	14.38
15	878.6	1.09	3657.0	1148.67	0	0	3	0	5.99	76.63	14.38
16	549.3	1.07	3657.0	356.68	0	0	3	0	5.99	76.63	14.38
17	437.5	1.05	3657.0	177.72	0	0	3	0	5.99	76.63	14.38
18	298.2	1.01	164.5	107.04	0	0	0	0	100	0	0
19	298.3	8.00	164.5	107.05	0	0	0	0	100	0	0
20	443.6	8.00	164.5	236.64	0	0	0	0	100	0	0

Table 4- *Results for layout 2*

Stream	T (k)	P (bar)	ṁ(gs^{-1})	Ėx (kW)	Molar fraction (%)						
					CH_4	CO	CO_2	H_2	H_2O	N_2	O_2
1	298.2	1.01	61.6	3221.00	100.00	0.00	0.00	0.00	0.00	0.00	0.00
2	390.7	2.94	61.6	3232.00	100.00	0.00	0.00	0.00	0.00	0.00	0.00
3	990.1	2.88	568.4	4892.00	15.13	5.78	22.50	11.19	45.40	0.00	0.00
4	850	2.88	568.4	4994.00	8.20	9.85	20.75	26.60	34.60	0.00	0.00
5	1130	2.82	777.8	2619.00	0.00	6.82	26.52	13.18	53.48	0.00	0.00
6	1130	2.82	506.8	1707.00	0.00	6.82	26.52	13.18	53.48	0.00	0.00
7	1130	2.82	271.0	912.80	0.00	6.82	26.52	13.18	53.48	0.00	0.00
8	298.2	1.01	3595.0	16.02	0.00	0.00	0.00	0.00	0.00	79.00	21.00
9	432.9	2.94	3595.0	431.30	0.00	0.00	0.00	0.00	0.00	79.00	21.00
10	761.4	2.88	3595.0	1038.00	0.00	0.00	0.00	0.00	0.00	79.00	21.00
11	870	2.82	3595.0	1307.00	0.00	0.00	0.00	0.00	0.00	79.00	21.00
12	1021	2.77	3595.0	1725.00	0.00	0.00	0.00	0.00	0.00	79.00	21.00
13	1130	2.82	3386.0	1949.00	0.00	0.00	0.00	0.00	0.00	83.38	16.62
14	1020	2.77	3386.0	1629.00	0.00	0.00	0.00	0.00	0.00	83.38	16.62
15	843.5	1.09	3386.0	893.80	0.00	0.00	0.00	0.00	0.00	83.38	16.62
16	501.7	1.07	3386.0	201.20	0.00	0.00	0.00	0.00	0.00	83.38	16.62
17	452.1	1.02	3386.0	121.00	0.00	0.00	0.00	0.00	0.00	83.38	16.62
18	298.2	1.01	206.2	0.92	0.00	0.00	0.00	0.00	0.00	79.00	21.00
19	298.2	1.01	50.3	5.24	0.00	0.00	0.00	0.00	0.00	5.00	95.00
20	410.6	2.73	50.3	9.93	0.00	0.00	0.00	0.00	0.00	5.00	95.00
21	1600	2.68	321.3	610.20	0.00	0.00	32.15	0.00	64.30	0.66	2.89
22	450	2.62	321.3	186.70	0.00	0.00	32.15	0.00	64.30	0.66	2.89
23	298.2	1.01	65.3	42.48	0.00	0.00	0.00	0.00	100.00	0.00	0.00
24	298.2	8.00	65.3	42.52	0.00	0.00	0.00	0.00	100.00	0.00	0.00
25	443.6	8.00	65.3	57.04	0.00	0.00	0.00	0.00	100.00	0.00	0.00

To find a better feature of the result for the two mentioned layout scenarios a comparison of the key features of the two cycles is presented in table 5.

Table 5- *Comparison of the two layouts*

	Layout 1	Layout 2	Exergy destructions (kW)	Layout 1	Layout 2
Net output power (kW)	1961	1902	After burner	191	78.77
SOFC power (kW)	1762	1749	Exhaust stream	177.7	121
Turbine power (kW)	704.6	680.9	SOFC	177.2	167.2
Air compressor power (kW)	-492.6	-492.6	Recuperator1	116.9	86.05
HRSG duty (kW)	438.6	174	Turbine	85.24	54.11
GT power (kW)	212	188.3	Recuperator2	80.36	50.56
Fuel compressor power (kW)	-13.51	-13.51	Air compressor	77.3	77.3
ASU power (kW)	-	-16.8	HRSG	49.37	65.64
Oxygen compressor power (kW)	-	-5.276	Mixer	45.82	46.96
Electrical efficiency (%)	63.47	61.57	ASU	-	87.26
Total efficiency (%)	77.67	67.20	Recuperator 3	-	5.37
Cell voltage (V)	0.7422	0.7366	Total exergy destruction	1009	840.22
HPR	22.37	9.152	EPC	68.66	73.67

In Table 6, some simulation results for these systems are compared with those quoted from previous studies (Kuramochi et al., 2007, Hill, 2003, Bavarsad, 2007, Motahar, 2008) to indicate the model accuracy. When the results are evaluated proportionally with their net output power, the differences between the published literature results and the presented models results are found to be in an acceptable range.

Table 6- *Comparison of some simulation results with literature*

	Layout 1(Presented paper)	(Bavarsad, 2007)	(Hill, 2003)	(Kuramochi et al., 2007)	(Motahar et al., 2008)
Air utilization factor (%)	25	18.8	45	36.32	22
Fuel utilization factor (%)	85	62.7	70	85	85
Fuel flow rate (g/s)	61.6	7.5	30.8	52	261
Air flow rate (g/s)	3595.4	582.9	1000	2092	17800
Steam to carbon ratio (SCR)	3	2.5	3	2	2.5
Average current density (A m^{-2})	3200	3200	N.A	N.A	3000
Number of cells	9456	1152	N.A	N.A	42624
Cell active area (m^2)	0.0834	0.0834	N.A	N.A	0.0834
Pressure ratio	2.9	2.9	8.5	4.5	9.9
Cell voltage (V)	0.7422	0.609	0.752	N.A	0.685
Cell operating pressure (bar)	2.76	2.88	7.9	4.12	9.9
Stack temperature (K)	1128.2	1273.15	1173.15	1263.3	1285.3
System exhaust temperature (K)	437.5	447.35	594.15	585.65	416.15
Net output power (kW)	1961	220.9	1039	1500	11641
SOFC power (kW)	1762	176.2	901.3	N.A	7300
GT power (kW)	212	46.86	166.8	N.A	5510
Electrical efficiency (%)	63.47	58.7	67.4	61.7	58.87
Total exergy destruction (kW)	1009	162.12	N.A	1050	3089.4

[1] Corresponding author: h.ghadamian@merc.ac.ir

ISSN : 0976-2876 (Print)

ISSN : 2250-0138 (Online)

To cover the comparison approach between layout 1 and layout 2, changes in the functional characteristics of the cycle and the key parameters such as output power, temperature and exergy are demonstrated as follow:

- As shown in table 5, the electrical efficiency of the layout 2 versus the layout 1 is reduced to 1.9% and the total efficiency is also reduced from 77.67 % to 67.20%. The main attributes for this reduction of electrical efficiency are the GT power loss ,due to decrease in turbine inlet temperature, and extra energy electrical consumption related to ASU unit that adds up to the cycle. Furthermore, the main reason for the reduction of the total efficiency is strongly dependent on HRSG consumption thermal energy which itself causes a reduction in inlet gas temperature.
- The most important segments with loss in exergy are: the SOFC contributed to electrochemical reactions, the after burner contributed to the combustion occurrence, the recuperators because of high temperature difference and the cycle' exhausted gas contributed to high temperature, respectively. Exergy destruction share for these layouts are shown in figures 4 & 5.
- The amount of saturate steam generated in the HRSG is 592.2 kg hr^{-1} and 235.08 kg hr^{-1} in the in layout 1 and layout 2, respectively. The main reason for the reduction in steam from HRSG in layout 2 is at the reduction of the inlet temperature.

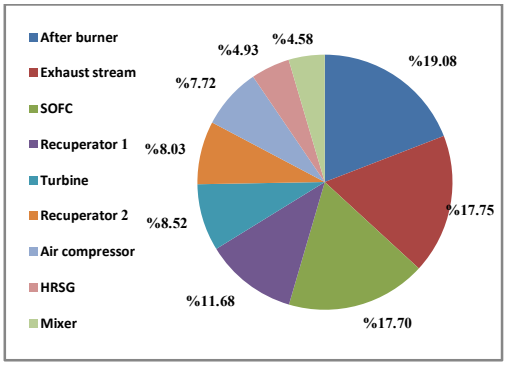

Figure 4- *Exergy destruction share for layout 1*

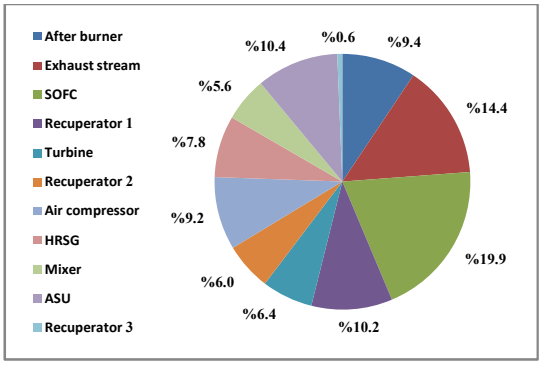

Figure 5- *Exergy destruction share for layout 2*

- Rated in net power output equal to 1961 kW in the layout 1, the amount of CO_2 produced by layout 1 is 169.4 g s^{-1} which corresponds to releasing 5342.20 tCO_2 $year^{-1}$ into the atmosphere. Specific CO_2 production in this cycle is 310.98 g kWh^{-1}. If compared with the CO_2 produced in conventional gas turbine power plants presented in reference (Hill, 2003) which was 367 g kWh^{-1}, so the present cycle is appealing15.26% reduction, to approve more increase in CO_2 capture rate, as an interest.
- Due to the addition of CO_2 capture module in the layout 2, this amount of CO_2 (equal to layout 1) is being capture and compressed at 90 bar pressure level which can be straight forward at the end users' services.
- Energy penalties related to equipment like oxygen compressor and ASU within CO2 capture module are considered in table 5. In other words, CO_2 compressing up to 90 bar pressure level will cause extra energy penalty equal to 58.16 kW in capacity and 1.81 % reduction in electrical efficiency. The mentioned values are individual concerns to provide CO_2 for end user delivery conditions, compared with the values conducted in table 5. As also shown in figure 2, with compression segment considerations, the electrical efficiency decreases from 61.57 % (showed in table 5) to 59.76 %. This reduction in efficiency is equal to 590.48 MWh annually.

[1] Corresponding author: h.ghadamian@merc.ac.ir

PARAMETRIC STUDY

In this section, regarding the input parameters, the effect of important parameters on the energy and performance of the two systems are investigated. Based on cycle characteristics, the U_f and RP are as variable keys of the cycles.

The cycle powers and HPR changes versus U_f in the layout 1 and layout 2 are shown in figures 6 and 8, respectively. Also the cycle efficiencies, EPC and cell voltage changes versus U_f in layout 1 and layout 2 are shown in figures 7 and 9 as well.

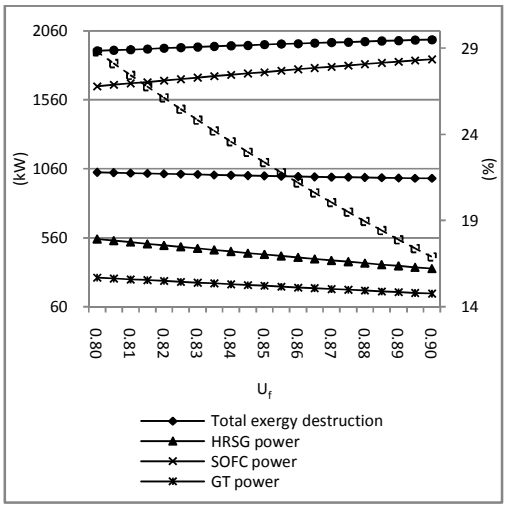

Figure 6- *Cycle powers and HPR changes in layout 1 versus U_f*

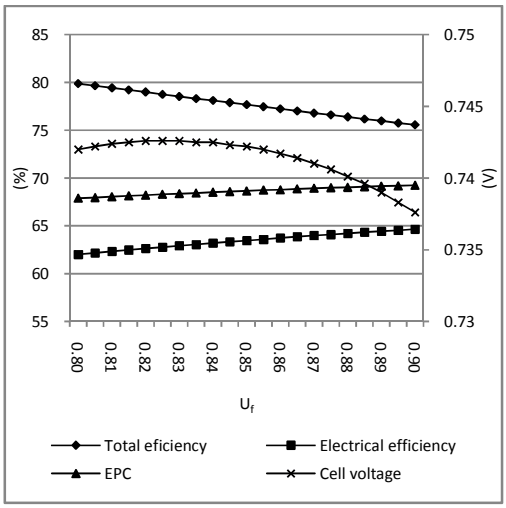

Figure 7- *Cycle efficiencies, EPC and cell voltage changes in layout 1 versus U_f*

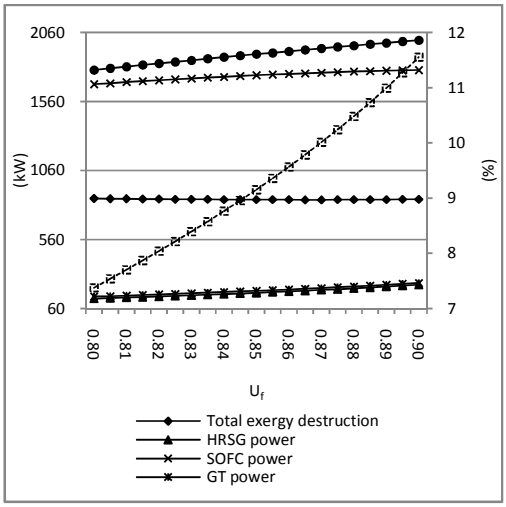

Figure 8- *Cycle powers and HPR changes versus U_f in layout 2*

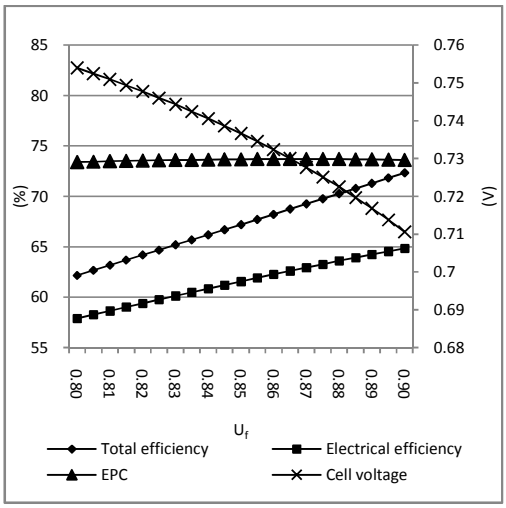

Figure 9- *Cycle efficiencies, EPC and cell voltage changes versus U_f in layout 2*

- As shown in figures 6 and 7, in the layout 1 cycle, increasing U_f has a positive impact on the electrical efficiency and EPC of the cycle and a negative impact on the total efficiency and HPR. Increasing the U_f causes increasing H_2 consumption in SOFC and thus increasing the SOFC power. In this case, the input fuel to after burner is reduced and leads to loss of electrical power and heat in GT and HRSG respectively. Increasing U_f more than U_f equal to 0.84, causes increasing of activation and ohmic voltage drops and thus reduces the cell

voltage. This phenomenon reduces the total efficiency of the layout 1 cycle. It should be noted that increasing net output power causes reduction in the total exergy destruction of the cycle.

- As shown in figures 8 and 9, in the layout 2, increasing U_f has a positive impact on the electrical and total efficiencies and also HPR of the cycle. It has a negative impact on the cell voltage and EPC. Increasing the value of U_f causes an increase in H_2 consumption in SOFC, in the same way as the layout 1, and thus increases the SOFC power. In this case, the SOFC operating temperature is increased. This leads to higher electrical power and heat production in GT and HRSG respectively. Increasing the value of U_f also causes an increase of activation and reduction of the ohmic voltage drops and thus reducing the cell voltage. This phenomenon increases the total efficiency of the layout 2. It should be mentioned that increasing the temperature differences in this cycle causes an increase in the total exergy destruction of the cycle.

The cycle powers and HPR changes versus RP in the layout 1 and layout 2 are shown in figures 10 and 11, respectively. Also the cycle efficiencies, EPC and cell voltage changes versus U_f in the layout 1 and layout 2 are shown in figures 12 and 13, respectively.

- As shown in figures 10 and 11, in the layout 1, there exists an optimal RP maximizing the electrical efficiency and EPC. In addition to that, the optimum point of energy efficiency and EPC are observed as RP increased. It is noteworthy to mention that the compressor pressure ratio maximizing the electrical efficiency and EPC and minimizing the HPR are different. When RP is 3.3, EPC touches its maximum value at 68.78 %. On the other hand, electrical efficiency is maximized at the RP equal to 3.5 and its value is 63.82 %. As well, the HPR is minimized at RP equal to 3.6 and its value is 21.2 %. It should be noted that increasing the RP causes an increase in SOFC operating pressure and thus increases the cell voltage.

- As shown in figures 12 and 13, in the layout 2, there is an optimal RP that maximizes the electrical efficiency and EPC and minimizes the HPR. Additionally, the compressor pressure ratio maximizing the electrical efficiency and EPC and minimizing the HPR are the same. When RP is 2.8, EPC reaches its maximum value at 73.68 %. The maximized electrical efficiency value is 61.58 %. As well, the minimized HPR value is 9.1 %. It should be noted that increasing the RP causes an increase in SOFC operating pressure and thus increases the cell voltage in the same way as the layout 1.

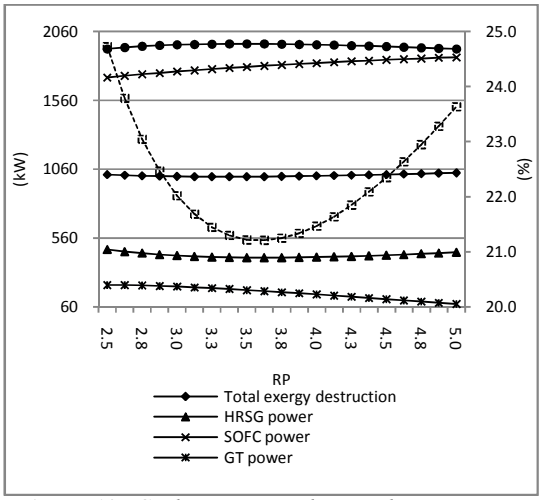

Figure 10- *Cycle powers and HPR changes in layout 1 versus RP*

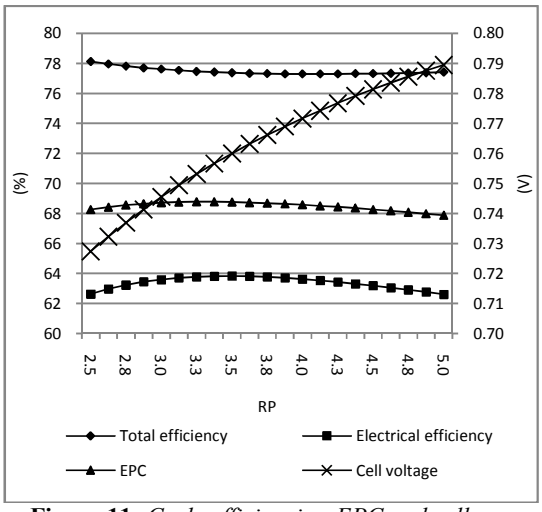

Figure 11- *Cycle efficiencies, EPC and cell voltage changes in layout 1 versus RP*

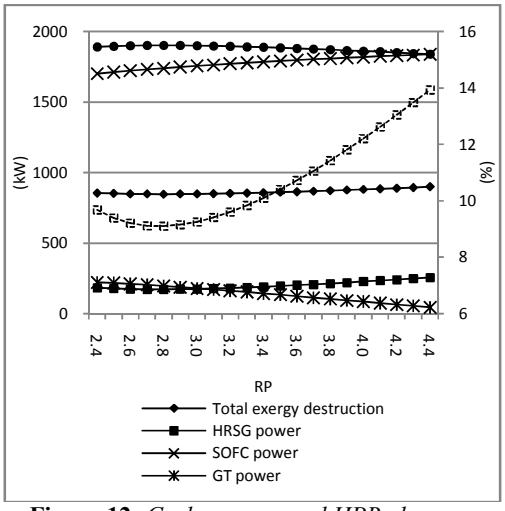

Figure 12- *Cycle powers and HPR changes versus RP in layout 2*

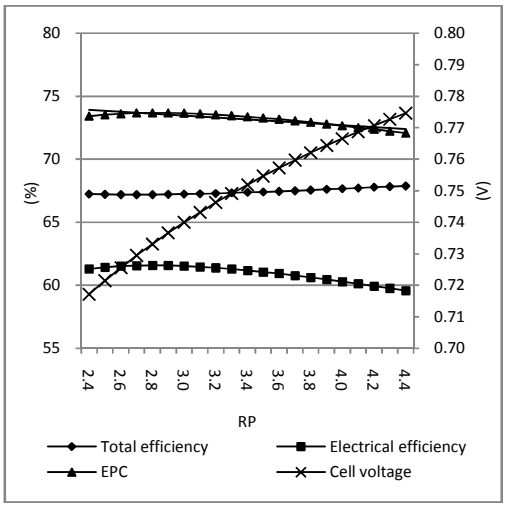

Figure 13- *Cycle efficiencies, EPC and cell voltage changes versus RP in layout 2*

CONCLUSION

Hybrid cycle of SOFC/GT with net output power 1961 kW, an electrical efficiency of 63.47%, the total efficiency of 77.67%, and output of 5342.20 tCO_2 $year^{-1}$ into the atmosphere performed a remarkable environmental aspect. Cycle scenarios comprising CO_2 capture module has led to achieve a cycle with proper CO_2 capture. However, at the same time the net output power was decreased to 1902 kW (equals to 3% power penalty). As a quantification approach, this degradation continued with electrical and total efficiency terms in decreasing order of 61.57% and 67.2%, respectively.

Total amount of exergy destruction equal to 1009 kW for layout 1, is reduced to 840.22 when we discussed in layout 2. By these means the EPC from 68.66 for layout 1 is changed to 73.67 for layout 2. Increasing in EPC, shows oppose to efficiency reduction the Layout 2 provide more proper design related to exergy considerations. In other word, 16.7% suitable decreasing in exergy destruction is taking place for layout 2, when it compares with layout 1 and EPC is increased 5.01% respectively.

In accordance with a parametric analysis, the changes in equipment power, exergy destruction, electrical efficiency, and EPC and cell voltage versus variables called U_f and RP with bounds of variations were compared. The results showed when U_f is 0.8, the total efficiency in layout 1 and EPC in layout 2 was maximized. When U_f is 0.9, the other items like the electrical efficiency, EPC in layout 1, total efficiency and electrical efficiency in layout 2, were maximized.

REFERENCES

http://iea.org/publications/freepublications/publication/name,31287,en.html

http://www.nfcrc.uci.edu/2/FUEL_CELL_INFORMATION/FCexplained/FC_Types.aspx

Singhal, S.C.; 2000. Advances in solid oxide fuel cell technology. Solid State Ionics. 135, 305–313.

Palsson, J. Selimovic, A. Sjunnesson, L.;2000.Combined solid oxide fuel cell and gas turbine systems for efficient power and heat generation.Journal of Power Sources. 86, 442–448.

Fuel cell handbook.; 2004. U.S. Department of Energy. 7th Ed.

Dennis, R.; 2007. The Gas Turbine Handbook (NETL, Morgantown).

Williams, G j. Siddle, A. Pointon, K.; 2001. Design Optimization of a hybrid Solid Oxide Fuel cell & Gas turbine power generation system. Alstom Power Technology centre.

Chan, S.H. Low, C.F. Ding, O.L.; 2002. Energy and Exergy analysis of simple solid oxide fuel cell power systems. Journal of Power Sources. 103, 188-200.

Calise F. Dentice M. Palomboa A. Vanoli L.; 2006. Simulation and exergy analysis of a hybrid Solid Oxide Fuel Cell (SOFC)– Gas Turbine System. Energy. 31, 3278–3299.

Akkaya, A.V. Sahin, B. Erdem, H.H.; 2007. Exergetic performance coefficient analysis of a simple fuel cell system, International Journal of Hydrogen Energy. 32, 4600 – 4609.

Haseli, Y. Dincer, I. Naterer, G.F.; 2008. Thermodynamic modeling of a gas turbine cycle combined with a solid oxide fuel cell. International Journal of Hydrogen Energy 33, 5811– 5822.

Gandiglio, M. Lanzini, A. Leone, P. Santarelli, M. Borchiellini, R.; 2013. Thermo economic analysis of large solid oxide fuel cell plants: Atmospheric vs. pressurized performance, J. Energy. In Press.

Saebea, D. Patcharavorachot, Assabumrungrat, Y. S. Arpornwichanop, A.; 2013.Analysis of a pressurized solid oxide fuel cell–gas turbine hybrid power system with cathode gas recirculation. International Journal of Hydrogen Energy. 38, 4748–4759.

Murphy, D.M. Richards, A.E. Colclasure, A. Rosensteel, Sullivan, W.A. N.P.; 2012.Biogas fuel reforming for solid oxide fuel cells. J. Renewable Sustainable Energy 4, 023106.

Ozgoli, H.A. Ghadamian, H. Roshandel, R. Moghadasi, M.; 2012. Alternative biomass fuels consideration exergy& power analysis for hybrid system includes PSOFC & GT integration. Energy Sources, Part A: Recovery, Utilization and Environmental Effects.

Kempegowda, R.S. Skreiberg, O. Tran, K.; 2012. Cost modeling approach and economic analysis of biomass gasification integrated solid oxide fuel cell systems. J. Renewable Sustainable Energy 4, 043109.

Ghadamian, H. Hamidi, A. A. Farzaneh, H. Ozgoli, H. A.; 2012.Thermo-economic analysis of absorption air cooling system for pressurized solid oxide fuel cell/gas turbine cycle, J. Renewable Sustainable Energy.4, 043115.

[1] Corresponding author: h.ghadamian@merc.ac.ir

Dijkstra, J. W. Jansen, D.; 2002. Novel Concepts for CO2 capture with SOFC. GHGT-6. Japan.

Bredesen R. Jordal K. Bolland O.; 2004. High temperature membranes in power generation with CO2 capture. Chemical Engineering and Processing. 43, 1129–1158.

Hanne, H. M. K. Jordal, K. Bolland, O.; 2007.A quantitative comparison of gas turbine cycles with CO2 capture. J. Energy. 32, 10–24.

Franzoni, L. Magistri, A. Traverso, A.F. Massardo.; 2008.Thermo economic analysis of pressurized hybrid SOFC systems with CO2 separation. J. Energy 33, 311–320.

Kuramochi T. Wu H. Ramirez A. Faaij A. Turkenburg W.; 2009. Techno-economic prospects for CO2 capture from a Solid Oxide Fuel Cell – Combined Heat and Power plant. Preliminary results. Journal of Energy Procedia. 1, 3843–3850.

Park, S.K. Kim, T.S. Sohn, J.L. Lee, Y.D.; 2011. An integrated power generation system combining solid oxide fuel cell and oxy-fuel combustion for high performance and CO2 capture. Applied Energy, 88, 1187–1196.

Hill, G.; 2003.Progress of the CO2 Capture Project (CCP) and Technology Development (BP).

Meyer, J. Mastin, J. Bjornebole, T.K. Ryberg, T. Eldrup, N.; 2011.Techno-economical study of the Zero Emission Gas power concept. Energy Procedia, 4, 1949–1956.

Adams, T.A. Nease, J. Tucker, D. Barton, P.I.; 2013. Energy Conversion with Solid Oxide Fuel Cell Systems: A Review of Concepts and Outlooks for the Short- and Long-Term. Ind. Eng. Chem. Res. 52, 3089−3111.

Arab, Gh. Ghadamian, H.; 2013.A technical assessment of the CO2 capture modeling for GT/SOFC/CHP hybrid cycles, (6th Iranian Fuel Cell Seminar, Tehran).

Kutas, TJ.; 1995. The exergy method of thermal plant analysis. Florida. Krieger Publishing Company.

Akkaya, A.V. Bahri, Erdem, S.; 2008.An analysis of SOFC/GT CHP system based on exergetic performance criteria, International journal of hydrogen energy. 33, 2566 – 2577.

Bavarsad, P. G.; 2007.Energy and exergy analysis of internal reforming solid oxide fuel cell–gas turbine hybrid system. International Journal of Hydrogen Energy.32, 4591–4599.

Motahar, S. Alemrajabi, A. A.; 2009.Exergy based performance analysis of a solid oxide fuel cell and steam injected gas turbine hybrid power system. International journal of hydrogen energy.1–12.